Published in final edited form as:
Phys Med Biol. 2014 August 7; 59(15): 4261–4273. doi:10.1088/0031-9155/59/15/4261.

Computing Proton Dose to Irregularly Moving Targets

Justin Phillips[1], **Gueorgui Gueorguiev**[1], **James A. Shackleford**[2], **Clemens Grassberger**[1], **Stephen Dowdell**[1], **Harald Paganetti**[1], and **Gregory C. Sharp**[1]

[1]Department of Radiation Oncology, Massachusetts General Hospital, Harvard Medical School, Boston, MA, 02114

[2]College of Engineering, Drexel University, Philadelphia, PA, 19104

Abstract

Purpose—While four-dimensional computed tomography (4DCT) and deformable registration can be used to assess the dose delivered to regularly moving targets, there are few methods available for irregularly moving targets. 4DCT captures an idealized waveform, but human respiration during treatment is characterized by gradual baseline shifts and other deviations from a periodic signal. This paper describes a method for computing the dose delivered to irregularly moving targets based on 1D or 3D waveforms captured at the time of delivery.

Methods—The procedure uses CT or 4DCT images for dose calculation, and 1D or 3D respiratory waveforms of the target position at time of delivery. Dose volumes are converted from their Cartesian geometry into a beam-specific radiological depth space, parameterized in 2D by the beam aperture, and longitudinally by the radiological depth. In this new frame of reference, the proton doses are translated according to the motion found in the 1D or 3D trajectory. These translated dose volumes are weighted and summed, then transformed back into Cartesian space, yielding an estimate of the dose that includes the effect of the measured breathing motion. The method was validated using a synthetic lung phantom and a single representative patient CT. Simulated 4DCT was generated for the phantom with 2 cm peak-to-peak motion.

Results—A passively-scattered proton treatment plan was generated using 6 mm and 5 mm smearing for the phantom and patient plans, respectively. The method was tested without motion, and with two simulated breathing signals: a 2 cm amplitude sinusoid, and a 2 cm amplitude sinusoid with 3 cm linear drift in the phantom. The tumor positions were equally weighted for the patient calculation. Motion-corrected dose was computed based on the mid-ventilation CT image in the phantom and the peak exhale position in the patient. Gamma evaluation was 97.8% without motion, 95.7% for 2 cm sinusoidal motion, and 95.7% with 3 cm drift in the phantom (2 mm, 2%), and 90.8% (3 mm, 3%)for the patient data.

Conclusions—We have demonstrated a method for accurately reproducing proton dose to an irregularly moving target from a single CT image. We believe this algorithm could prove a useful tool to study the dosimetric impact of baseline shifts either before or during treatment.

Keywords

4D treatment planning; irregular breathing; proton therapy; baseline drift

I. INTRODUCTION

Many strategies exist to mitigate the effect of irregular motion[1], including the breath hold technique[2,3], active breathing control[4] and respiratory gating[5,6]. These options are not always feasible for patients, especially those in advanced stages of disease. In addition, patients with sufficiently small tumor motion who are not candidates for motion mitigation can still exhibit unexpected irregular motion during treatment. To account for these uncertainties, treatment planning must be performed on images taken over the entire respiratory cycle. Estimating the effects of motion on the dose distribution has been explored for years[7], and methods have been designed to reconstruct dose data for treated tumor positions not captured by imaging[8,9,10]. However, most effort in this area has been spent in photon therapy. Our proposed method is a novel approach designed specifically to address the need for the same error calculations for proton therapy.

Proton therapy can be a highly effective modality for radiotherapeutic treatment because of the high conformality offered due to the physical properties of protons[11]. However, the characteristics that allow proton beams to improve local control by sparing healthy tissue and more precisely target tumors also complicate dose calculations for moving targets. Because the proton's range depends on the tissues it traverses, a targeted tumor that moves due to respiration can produce dramatic shifts in the dose distribution[12]. The change in the dose to surrounding tissue and critical structures for a single respiratory cycle can be computed with data from four-dimensional computed tomography (4DCT), but if the tumor strays outside the imaged range of motion during treatment, it is much more difficult to accurately estimate the dose.

Techniques using 4DMRI to deformably reconstruct CT data[13,14] have found success in addressing this issue, provided that dense 4D imaging data is available. Other studies have presented calculations of RBE-weighted doses[15] and assessed the effects of interplay and motion mitigation techniques on a patient-specific basis[16]. These analyses require full 4DCT data and recomputation of dose distributions.

Our motivation is a fast method that can be applied to both passively scattered and pencil beam dose plans, needs only 3DCT data, and does not require treatment planning software for dose calculation. The capability to compute dose to surrounding tissue without requiring CT data would be an asset, as CT images at every position during treatment are not always available. An algorithm that uses existing CT data to extrapolate dose calculations to unrecorded tumor positions would allow a planner to make informed interfraction treatment plan corrections based on this feedback. In addition, using these exisiting dose calculations to derive results eliminates the need for access to treatment planning software. Finally, it is highly desirable to assess the dosimetric impact of baseline shifts during respiration, as this would allow treatment planners to better estimate dose and assess patient-specific treatment margins. A fast algorithm would allow planners to perform intrafractional corrections, as well as study large volumes of patient data between treatments.

In this study, we provide an accurate estimate of dose delivered to an irregularly moving target with a limited amount of CT data, while meeting the needs stated above. The method

was tested using unfavorable setup conditions to illustrate the proof of concept. This included using data with large degrees of lung tumor motion, and limiting our data set to only one CT image for the dose calculation. The method was performed with multiple simulated breathing patterns on both a digital phantom and patient data. Through gamma analysis, we assessed the accuracy of this approximation against a ground truth dose created through deformable registration.

II. MATERIALS AND METHODS

A. Concept

Due to respiratory motion, it is not necessarily straightforward to compute the accurate dose delivered to a moving tumor and surrounding tissue. When calculating dose from a photon beam, the change in dose over each phase of a 4DCT due to shifting anatomy is comparably smaller than that of protons. Because the depth distribution of a photon beam in tissue is characterized by a mass-dependent linear attenuation, it remains somewhat insensitive to longitudinal shifts in anatomy that occur during breathing. While models sometimes neglect the dose differences due to these longitudinal variations, transverse motion can have a more signficant impact on the dose distribution. However, due to the comparatively smaller impact of range effects from photons, this issue has been well explored[8,9,10]. As the configuration remains morphologically static over each phase, one can estimate the dose delivered by the field to the moving tissue by convoluting and summing a single dose calculation over the range given by a respiratory motion function. As a result, only one CT image and accompanying dose is required to estimate a reasonably accurate composite dose for photons in this manner. However, for protons, this method is not feasible. Due to range effects of charged particles and the Bethe-Bloch dependence on the density of the stopping material, the shape of a given proton dose cloud is dependent on the tissues that it passes through. Thus, a targeted tumor that moves due to respiration can produce dramatic shifts in the dose distribution. To obtain an accurate assessment of the total dose, one must perform a new calculation over each tumor position.

When the goal is to compute dose to a moving target and surrounding tissue, it is convenient to reason in a tumor-centric coordinate system. As seen in an example in Figure 1, dose distributions have been calculated with the same beam settings on the two different CT images containing a tumor at the exhale and inhale positions. To achieve this transformation, we translate or deform the entire 4DCT set into one reference phase, such that the tumor center is located at the same coordinate in each image. In Figure 1, we have chosen the mid-ventilation point as the reference frame, and translated the two CT images and doses correspondingly. When the total is summed, this allows us to obtain the total dose delivered to the target and surrounding tissue, as shown in the final image.

An accurate assessment of the dose delivered to a regularly moving target can be performed with the above procedure. This calculation is dependent on utilizing a full 4DCT set that encompasses the entire range of tumor motion during treatment. However, the tumor location during treatment can vary greatly compared to the location recorded during simulation. If this occurs and the tumor position during treatment strays outside the bounds

of the imaging CT set, there is no way to directly calculate the dose delivered at this position.

One approach to indirectly compute dose around a tumor at an unimaged position is to translate the beam and recalculate the dose distribution on an existing CT image. The magnitude of the beam displacements can be derived from the recorded breathing function, allowing one to first compute the dose at each position, then appropriately weight and sum the results in the aforementioned tumor-centric frame. However, this method requires a new dose calculation at each beam location, which can be time-intensive and requires access to treatment planning software with advanced capability.

By designing the Water-Equivalent Depth (WED) method, our goal was to approximate a solution for this issue. An existing image is chosen, ideally from a 4DCT phase as close in position as possible to the missing tumor locations. This algorithm uses that CT to convert previously calculated dose volumes from their original Cartesian geometry into a beam-specific radiological depth space. After a dose is warped into this new space, the resulting distribution is shaped as if the proton cloud were only interacting with a homogeneous medium composed of water. In this coordinate system, we can translate the proton dose distributions in the same way as with photons in the previously mentioned method. By mitigating the impact of the proton range effects in this manner, we reconstruct dose contributions from any missing target position in the recorded treatment signal by translating existing dose clouds in this water-equivalent depth space. While the presented results test only beams generated through passive scattering, this method can also be applied to spot scanning plans, provided that the timing of each pencil beam relative to the recorded breathing pattern is known.

B. Software Design

As shown in Figure 2, the algorithm can be broken down into four steps. To begin, the required inputs are a CT image used to generate the conversion matrix into WED space and a reference dose calculated on that CT to be warped. The new WED frame of reference is beam specific, converting the chosen CT image into a radiological depth space with the longitudinal direction determined by the source-isocenter vector. The axes are parameterized by the dimensions and resolution of a grid overlaid on the aperture and the corresponding source location. This geometry establishes the new coordinate system, in which each ray is parameterized into 2D space based on the transverse location of intersection with the aperture. While the transverse axes in the WED coordinate system map the projection of the aperture opening in beam's eye view and are unitless, they can be approximated as the geometric transverse distances for beams with small divergence. The longitudinal axis in this new space is characterized by the radiological depth, generated by tracing each ray and recording the corresponding geometric distance traveled for each unit of radiological distance. This conversion matrix can be used to warp any image, including a dose volume, overlaid on the original CT into WED space as shown in Figure 2a.

The second step (Figure 2b) takes place within the WED coordinate system. Assuming one has warped the desired dose (or doses), each can be translated using the projected tumor center locations within the 2D aperture plane for each phase. In the third step (Figure 2c),

the composite dose in WED space is constructed from summing the translated doses using weightings generated from the tumor motion waveform.

The final step is the conversion of the summed result from WED space back into geometric coordinates (Figure 2d). The same conversion matrix and corresponding ray geometry is used in an inverse transformation of the WED dose. Each voxel in the reconstructed geometric volume is derived from a trilinear interpolation using values from the nearest four projective rays. Data loss necessarily exists in the conversion from Cartesian to WED space, but does not occur in this inverse transform.

The software for the proposed technique was developed within Plastimatch[17], an open source toolkit designed for image registration and manipulation. Plastimatch allows for the conversion between file types used in medical imaging research, including the DICOM and ITK[18] images used in this project. With the exception of the original importation of the patient data in DICOM format, all image manipulation was performed within ITK structures.

C. Phantom

Validation tests used digital phantoms created for this project. These phantoms were created using an in-house simulator written in Matlab. Shown in Figure 3, the phantom mimicked a 4DCT of a moving tumor in a simplified lung geometry, containing an outer, 30 mm thick cylindrical shell of water (0 HU) surrounding the inner tissue volumes. This layer enclosed a cylinder with radius 50 mm of lung tissue (-700 HU), and a spherical tumor (-300 HU) with radius 15 mm was located at several positions along the axis within the lung. A total of 26 volumes representing different phases were created with the tumor locations at 2 mm intervals, ranging between [-3, 2 cm] from the mid-ventilation point.

D. Patient data

One patient CT was selected from a data set of lung cancer cases used in Monte Carlo studies under IRB approved protocol[19]. The patient was imaged at Massachusetts General Hospital (MGH), receiving treatment for a tumor in the left lung. The centroids of the tumor were measured manually and used to generate the axial o sets needed for the translations in WED space. The full range of craniocaudal motion was 8.0 mm, with less than 3.5 mm of transverse displacement in the other planes. In addition to testing the WED output against ground truth, we also performed a simplified, naive calculation that convolves the input dose with the breathing function in Cartesian space as a baseline test.

E. Treatment Planning

A treatment plan for the digital phantom was designed based on the mid-ventilation CT, using a protocol from MGH[20]. From the contoured GTV, a CTV was obtained by applying a uniform 7 mm expansion. To determine the ITV, the protocol dictated a nonuniform expansion of the CTV along the direction of motion, with the longitudinal dimension determined by the peak-to-peak distance of the respiratory motion. This resulted in an ITV with a length of 22 mm in the axial direction and 8 mm in the transverse directions.

For the patient treatment plan, an IGTV was derived from a maximum intensity projection (MIP) of each phase, and then validated for motion coverage on the 4DCT. The ITV used for treatment planning was generated from a 5 mm expansion of the IGTV. The apertures and compensators were designed to deliver 95% ITV coverage, resulting in additional 6 mm and 5 mm margins for the phantom and patient plans, respectively. The phantom dose was calculated with XiO[21], and the patient dose was calculated using TOPAS[22].

F. Ground Truth Calculation

For both the phantom and patient data, we calculated the dose distribution on each 4DCT image, and then warped each result into a tumor-centric coordinate frame. We then summed them in this frame with weightings derived from each tumor motion waveform. With this procedure, we can derive the ground truth for any irregular breathing pattern, as long as tumor positions in the 4DCT remain within the bounds determined by the breathing signal. For the digital phantom, we accumulated dose by translating each calculation by the corresponding CT's tumor displacement from the reference position at exhale (T50). In computing the patient data, deformable registration with Plastimatch was used to bring each computed dose into the reference frame.

On the phantom data, doses were accumulated according to two motion trajectories. Two sinusoids were generated with an amplitude of 2 cm, with one of these signals including a 3 cm drift over the measurement period, as shown in Figure 4. The motion waveforms were binned into histograms with 2 mm width, corresponding to the phantom CT volumes with equivalently spaced tumor locations. These results were used both to construct the ground truth and to weight the doses in WED space before adding them and converting the summed result back into Cartesian coordinates.

For the patient data, because every CT was deformably registered into the same exhale reference phase, each respective warped dose was generated into a common, tumor-centric coordinate system. While the relevant weightings were still applied, the warped doses were added in the same frame of reference with no additional o sets. When constructing the patient dose, we did not use a synthesized motion signal, but rather assigned an equal weighting to each phase for the ground truth and WED calculations.

III. RESULTS

Once the tumor motion signals were used to accumlate the dose distributions, we applied the WED algorithm to reconstruct the ground truth. For each phantom, we computed a beam-specific WED volume, and from this computed the expected dose from that beam including motion. The results were quantified using gamma analysis and tabulated in Table I.

A. Phantom

We tested the algorithm using three configurations of the phantom data. First, to function as a control, we took a single dose distribution at the mid-ventilation phase, converted it into WED space, and reconstructed it back into Cartesian space. The dose was not translated and summed in the WED coordinate frame as we would do if we were constructing a tumor motion signal (Figure 2c), since the goal was to use the simplest possible set of

transformations and recover the intial dose by applying the conversion matrix followed by its inverse. This test assesses the amount of data lost in the linear interpolations used in the warping process and characterizes the algorithm's performance.

Figure 5 (left) displays the ground truth dose, the WED computed dose, and the gamma distribution with a global gamma index of 97.8% (for 2 mm, 2%, 10% cuto). In the central high dose region, the dose is predictably reproduced with minimal differences from the ground truth. Towards the edge of the distribution where the dose gradient is steepest, the reconstruction suffers the most from interpolative data loss.

The second configuration estimates the dose expected from the sinusoidal signal of Figure 4. As before, only the mid-ventilation dose and CT were used in the computation. The converted dose and WED-normalized CT image of the phantom can be seen in Figure 3. Axial and sagittal views of the phantom with the mid-ventilation dose are seen on top (left and right, respectively), with the corresponding WED converted volumes on the bottom. A notable feature from the warped geometry is the reduction of the lung volume and associated dose relative to the other tissues.

The midventilation WED-converted dose was copied, translated, and assigned a weight based on the sinusoidal input signal. This step is analogous to the generation of the ground truth composite doses, but as shown in Figure 2b, is computed in WED space. The result was converted back into Cartesian space, and we obtained a gamma of 95.7% compared to ground truth. As can be seen in Figure 5, the algorithm performs more poorly near both the steeper dose gradients and density changes within the CT.

The last configuration we tested with the phantom used the sinusoidal signal with an added drift (shown in Figure 4).

Ground truth and WED estimated dose were constructed in the same manner as the sinusoid without drift, using only the WED-converted mid-ventilation dose translated over 26 tumor positions. Shown in the right column of Figure 5, the gamma distribution exhibits similar features to the previous results. As expected, the dose distribution is asymmetric along the superior-inferior direction, with more high dose volume inferior to the midpoint. In tumor-centric coordinates, this results in more dose being delivered to the moving tissue superior to the tumor. We obtained a gamma result of 95.7% for this experiment.

B. Patient

The procedure to test the WED algorithm on the patient data followed the same steps used for the phantom. However, instead of translating the dose, the ground truth used for the gamma comparison was constructed with deformable registration.

The patient analogue to the phantom of Figure 3 is shown in Figure 6. As before, two slices transverse to the beam are shown with isodose lines of the simulated dose overlaid. The beam for this plan is oblique, with a gantry angle of 160 degrees. Thus, of the two transverse CT images shown, one is along the $\hat{z}$ (axial slice, on the left) and the other has both x $\hat{}$ and $\hat{y}$ components (on the right). These two vectors parameterize the transverse axes for the WED

coordinate system used to create the transformation matrix in this calculation, and the resultant warped CT and dose are shown below the original CT images. Noteworthy features in the warped CT's include the markedly decreased lung volumes, the tumor (the warped mass within the isodose lines), and bony landmarks such as the spine and ribs that increase in volume.

Results for the patient dose calculation are shown in Table I. In this case, our reference phase was at peak exhale, and like the mid-ventilation dose for the phantom, we translated and accumulated the corresponding WED-converted dose. After converting the result back into Cartesian space, we achieved a global gamma index of 90.8% (3 mm, 3%).

Finally, one should be aware that comparing large, homogeneous dose volumes in lung tissue can result in overly generous gamma values. We included a straightforward “naive” calculation, to provide context for the performance of the WED method. We translated and summed the reference exhale dose in Cartesian space using the measured o sets, disregarding proton range effects from the CT data. This experiment resulted in a gamma of 69.1%.

IV. DISCUSSIONS AND CONCLUSIONS

This study has demonstrated a robust method for calculating proton dose with limited amounts of CT data. In general, we attempted to use minimal amounts of CT and dose data, and evaluate the results in scenarios with large motion. With a single CT and an accompanying dose calculation, this method allows one to estimate the dosimetric impact of motion on a delivered treatment for any tumor position signal. In each of the examples demonstrated above, we used only one phase to extrapolate the entire dose. The mid-ventilation phase was used in the phantom calculations, while the exhale phase was chosen as the reference for the patient data due to its characteristic stability when using deformable image registration. However, in a clinical setting, one would prefer to use as much of the original CT information as possible in calculating the total dose, while using the WED method to reconstruct contributions from any recorded tumor positions that lacked imaging data.

Consider a case in which we had pre-treatment 4DCT data of a tumor with 2 cm motion, but the breathing signal during treatment indicated that the tumor moved 3 cm. A sensible approach would be to compute dose on all 4DCT phases. Then, one could use the WED algorithm on the CT image closest to the missing positions within the full 3 cm range of motion to extrapolate the remaining contribution.

Certain features of the gamma distributions merit discussion. First, each treatment plan was designed to target a tumor surrounded by lung tissue, which is roughly three times less dense than water. Any margins used in both protocols to ensure distal and proximal coverage are water-equivalent. This results in a much greater geometric margin in lung tissue. As can be seen in Figures 5 and 7, each tumor-centric dose calculation has a central region that is lareg, homogeneous, and easily reproducible by the WED algorithm. Because the ratio of this volume to that with the more difficult penumbra is relatively large, the gamma criteria

returns a higher score. One should keep this in mind when comparing doses in lung, and we plan to further address this in our future work.

Second, as shown in Figure 7, the ground truth dose clearly differs from the WED dose near the skin. This behavior was expected, as deformable registration was used to create the ground truth tumor-centric dose. Because the WED method is designed to account for proton range effects and uniformly translates the converted dose to follow tumor motion, disparities are expected in regions that do not strictly translate. This highlights a limitation of the WED technique, as its accuracy is limited in tissue proximal to the target that does not follow the same pattern of motion (such as ribs or skin). While this algorithm is not currently designed to handle deformation, one could account for sliding motion across an interface with this method by holding the desired contoured volumes static in the WED frame of reference while the remaining warped CT was translated. While this restriction should be recognized and taken into account, it should be reiterated that the purpose of this technique is the calculation of dose to moving tissue and OAR's near the target. Also of note, another weakness of this method is that laterally scattered dose due to multiple coulomb scattering is only accurate when the depth is relatively constant.

We have demonstrated a proof of concept that can be applied to clinical routine. To our knowledge, there is currently no other method that accurately estimates dosimetric impact of a proton treatment plan with limited CT data. This algorithm is accurate, simple to implement, and takes minimal computation time. For these reasons, we believe that the WED method would be a powerful clinical tool to study the effect of irregular breathing motion before or during treatment.

Acknowledgments

This work was supported by NCI under R01 CA111590.

References

1. Keall, Paul J.; Mageras, Gig S.; Balter, James M.; Emery, Richard S.; Forster, Kenneth M.; Jiang, Steve B.; Kapatoes, Jeffrey M.; Low, Daniel A.; Murphy, Martin J.; Murray, Brad R., et al. The management of respiratory motion in radiation oncology report of AAPM Task Group 76. Medical physics. 2006; 33:3874. [PubMed: 17089851]
2. Dale Kubo H, Len Patrick M, Minohara Shin-ichi, Mostafavi Hassan. Breathing-synchronized radiotherapy program at the University of California Davis Cancer Center. Medical physics. 2000; 27:346. [PubMed: 10718138]
3. Jiang, Steve B. Seminars in radiation oncology. Vol. 16. Elsevier; 2006. Radiotherapy of mobile tumors.; p. 239-248.
4. Wong JW, Sharpe MB, Jaffray DA. The use of active breathing control (ABC) to reduce margin for breathing motion. Int. J. of Radiation Onocology Biology Physics. 1999; 44:911–919.
5. Margeras GS, York E. Deep inspiration breath hold and respiratory gating strategies for reducing organ motion in radiation treatment. Seminars in Radation Oncology. 2004; 14:65–75.
6. Ford EC, Mageras GS, Yorke E, Rosenzweig KE, Wagman R, Ling CC. Evaluation of respiratory movement during gated radiotherapy using film and electronic portal imaging. International Journal of Radiation Oncology* Biology* Physics. 2002; 52(2):522–531.
7. Bortfeld T, Jiang SB, Rietzel E. Effects of motion on the total dose distribution. Seminars in Radation Oncology. 2004; 14:41–51.

8. Lujan, Anthony E.; Larsen, Edward W.; Balter, James M.; Ten Haken, Randall K. A method for incorporating organ motion due to breathing into 3d dose calculations. Medical physics. 1999; 26:715. [PubMed: 10360531]
9. Chetty I, et al. A fluence convolution method to account for respiratory motion in three-dimensional dose calculations of the liver: A Monte Carlo study. Med. Phys. 2003; 30
10. Chetty I, et al. Accounting for center-of-mass target motion using convolution methods in Monte Carlo-based dose calculations of the lung. Med. Phys. 2004; 31
11. Chang, Joe Y.; Zhang, Xiaodong; Wang, Xiaochun; Kang, Yixiu; Riley, Beverly; Bilton, Stephen; Mohan, Radhe; Komaki, Ritsuko; Cox, James D. Significant reduction of normal tissue dose by proton radiotherapy compared with three-dimensional conformal or intensity-modulated radiation therapy in Stage I or Stage III non-small-cell lung cancer. International Journal of Radiation Oncology* Biology* Physics. 2006; 65(4):1087–1096.
12. Mori, Shinichiro; Wolfgang, John; Lu, Hsiao-Ming; Schneider, Robert; Choi, Noah C.; Chen, George TY. Quantitative assessment of range fluctuations in charged particle lung irradiation. International Journal ofRadiation Oncology* Biology* Physics. 2008; 70(1):253–261.
13. Boye, Dirk; Lomax, Tony; Knopf, Antje. Mapping motion from 4d-mri to 3d-ct for use in 4d dose calculations: A technical feasibility study. Medical physics. 2013; 40(6):061702. [PubMed: 23718581]
14. Zhang, Ye; Knopf, A.; Tanner, C.; Boye, D.; Lomax, AJ. Deformable motion reconstruction for scanned proton beam therapy using on-line x-ray imaging. Physics in medicine and biology. 2013; 58(24):8621. [PubMed: 24256693]
15. Gemmel A, Rietzel E, Kraft G, Durante M, Bert C. Calculation and experimental verification of the rbe-weighted dose for scanned ion beams in the presence of target motion. Physics in medicine and biology. 2011; 56(23):7337. [PubMed: 22048526]
16. Kraus KM, Heath E, Oelfke U. Dosimetric consequences of tumour motion due to respiration for a scanned proton beam. Physics in medicine and biology. 2011; 56(20):6563. [PubMed: 21937770]
17. Sharp G, et al. Plastimatch - An open source software suite for radiotherapy image processing. Proceedings of the XVIth International Conference on the use of Computers in Radiotherapy. 2010
18. Ibanez, L.; Schroeder, W.; Ng, L.; Cates, J. The ITK Software Guide. second edition. Kitware, Inc.; 2005. ISBN 1-930934-15-7, http://www.itk.org/ItkSoftwareGuide.pdf
19. Grassberger, Clemens; Dowdell, Stephen; Lomax, Antony; Sharp, Greg; Shackleford, James; Choi, Noah; Willers, Henning; Paganetti, Harald. Motion interplay as a function of patient parameters and spot size in spot scanning proton therapy for lung cancer. International Journal of Radiation Oncology* Biology* Physics. 2013; 86(2):380–386.
20. Engelsman, Martijn; Rietzel, Eike; Kooy, Hanne M. Four-dimensional proton treatment planning for lung tumors. International Journal of Radiation Oncology* Biology* Physics. 2006; 64(5): 1589–1595.
21. Proton, XiO. version 4.2.1. Elekta AB; Stockholm, Sweden: 2013.
22. Perl J, et al. TOPAS: An innovative proton Monte Carlo platform for research and clinical applications. Med. Phys. 2004; 39

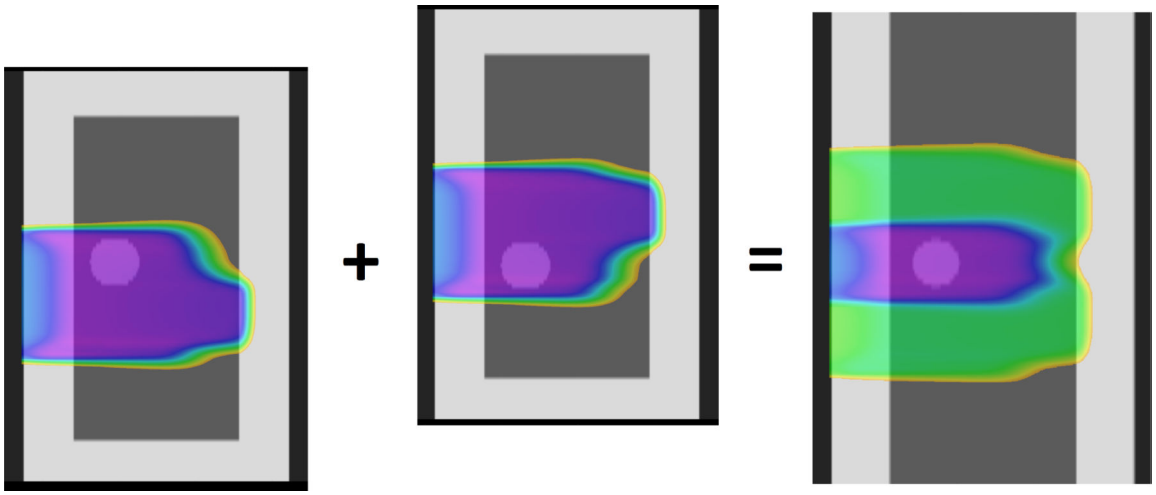

FIG. 1.

Example dose addition of inhale (T00) and exhale (T50) phases in a tumor-centric coor dinate system.

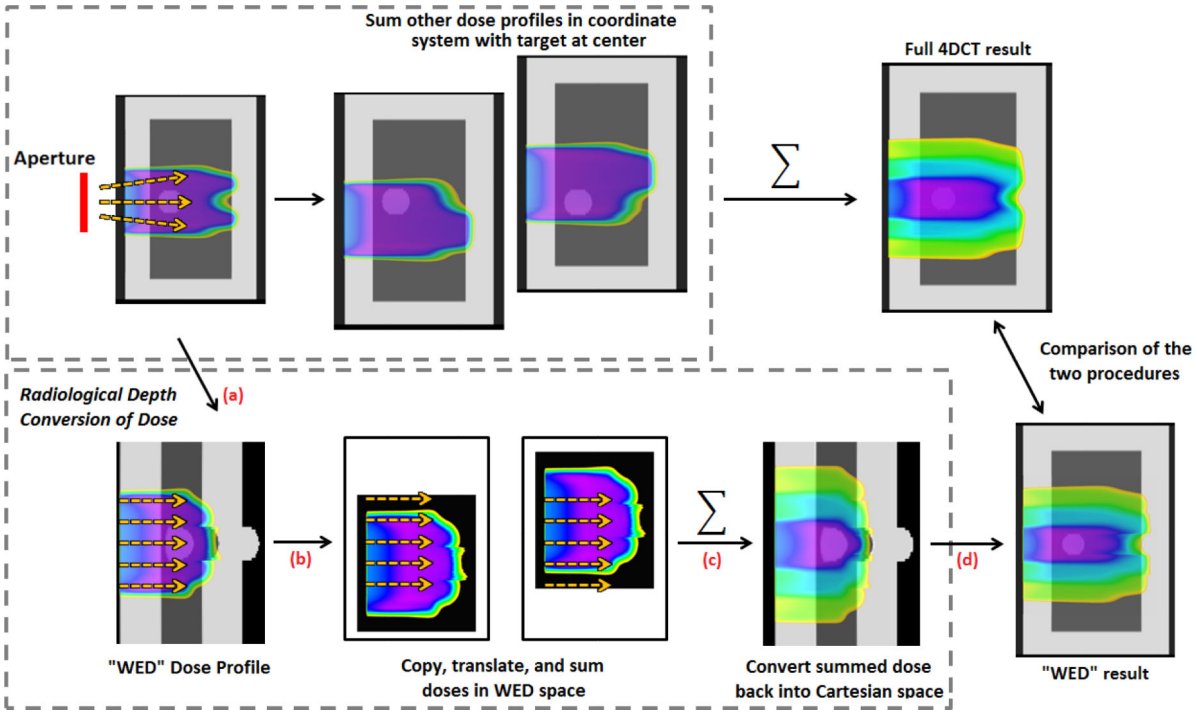

FIG. 2.

Flow chart showing each step of the WED process.

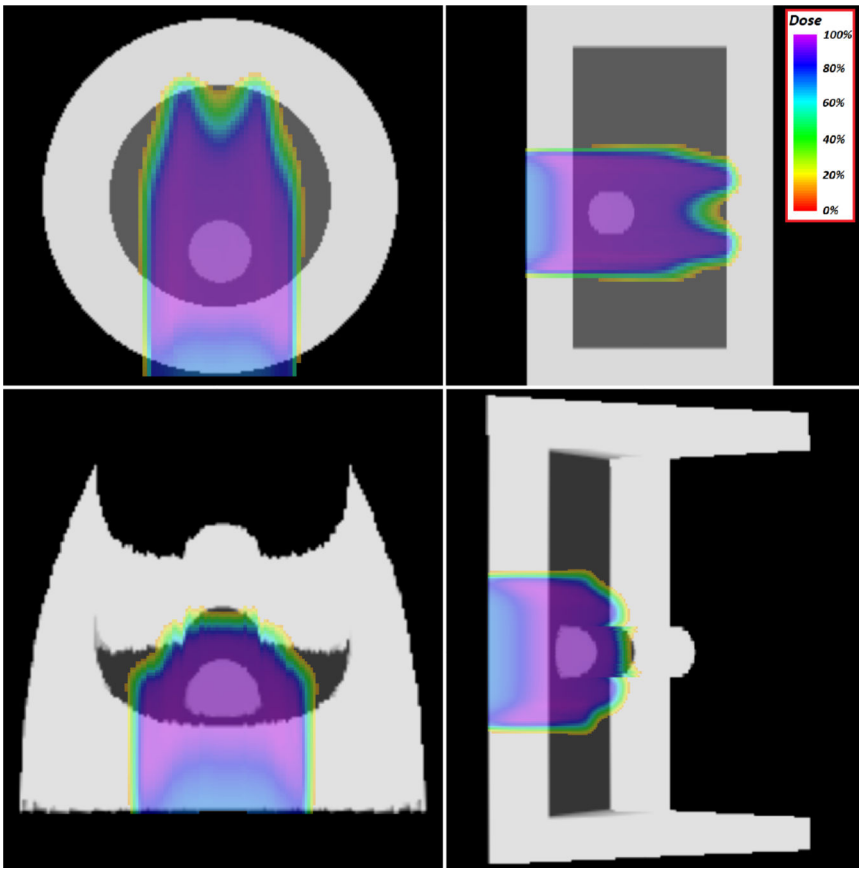

FIG. 3.

(Top) Axial and sagittal views of cylindrical phantom with accompanying dose distribution. (Bottom) WED conversion of both phantom and dose, using the projective rays from the aperture as determined by the dose plan.

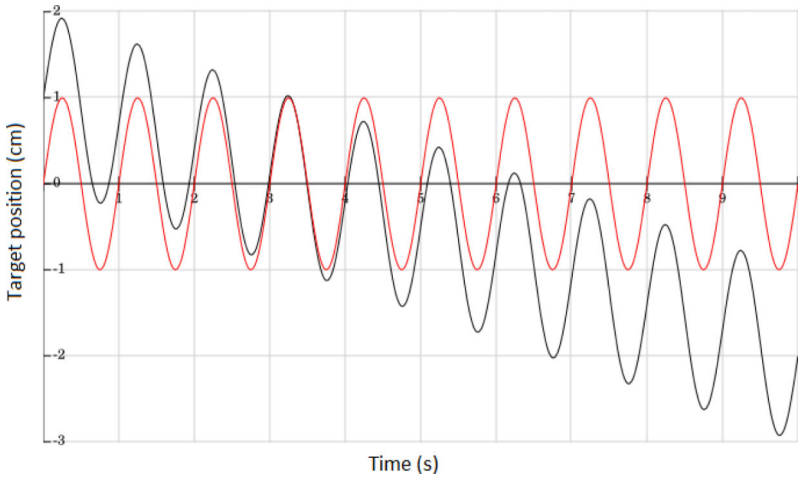

FIG. 4.

Simulated breathing functions used to weight WED generated dose clouds across each phase of the phantom. Both are sinusoids with peak-to-peak amplitudes of 2 cm. One (red) contained no baseline drift, while the the other (black) included a 3 cm shift over the measurement period.

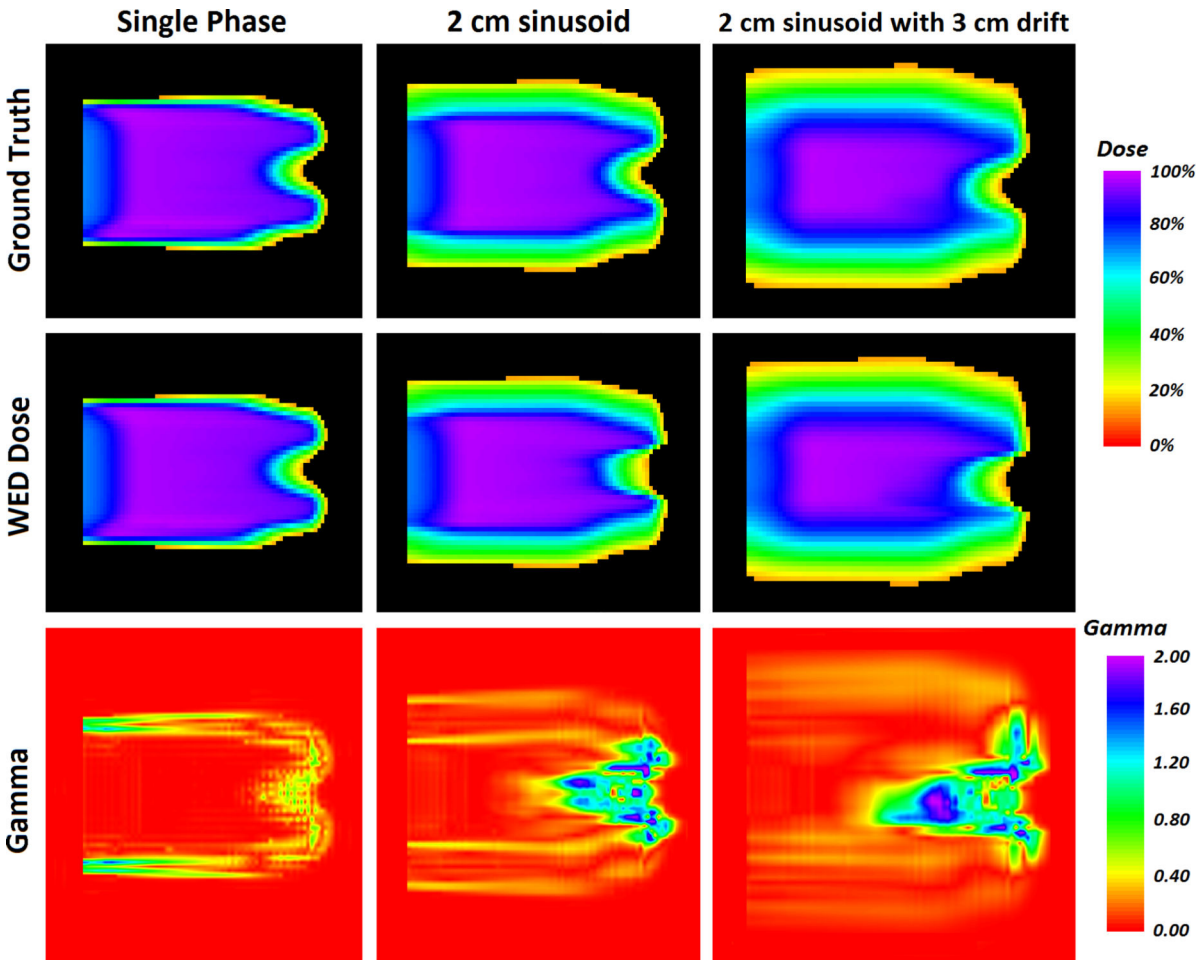

FIG. 5.

Dose and gamma plots of the three WED calculations using the phantom. On this grid, shown from left to right are the single phase, sinusoid, and sinusoid with drift results. From top to bottom are the ground truth dose distributions, the doses reconstructed using the WED method, and the global gamma analyses between both (2 mm, 2%).

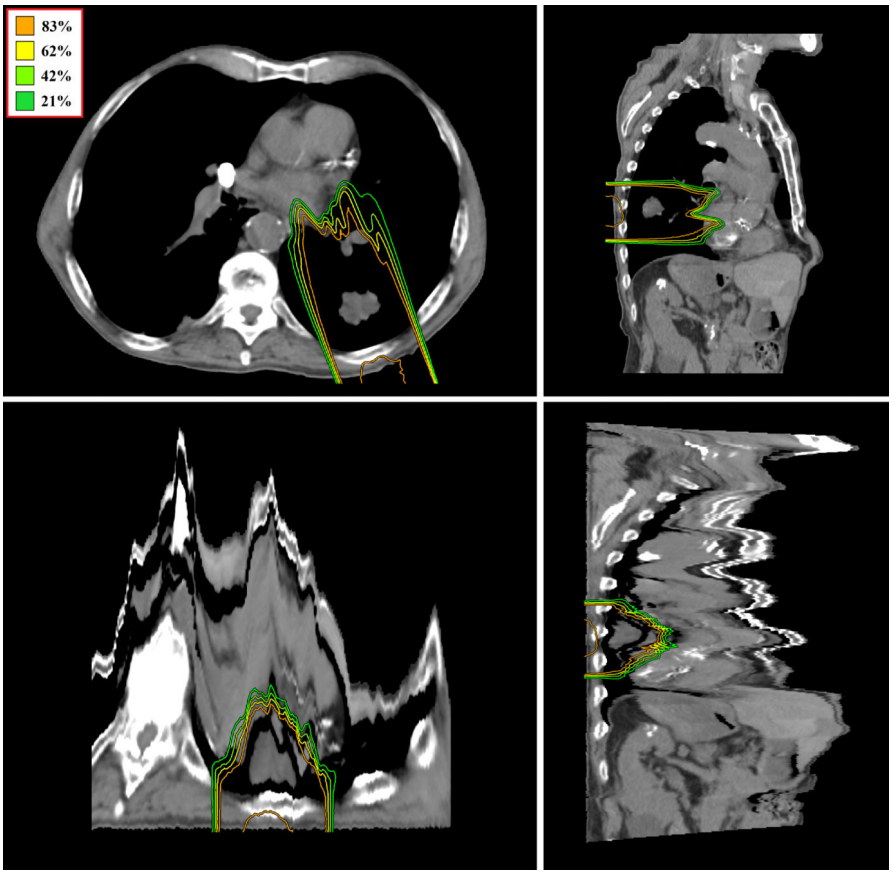

FIG. 6.

(Top) Axial and sagittal views of patient CT with isodose lines. (Bottom) WED conversion of both CT and dose.

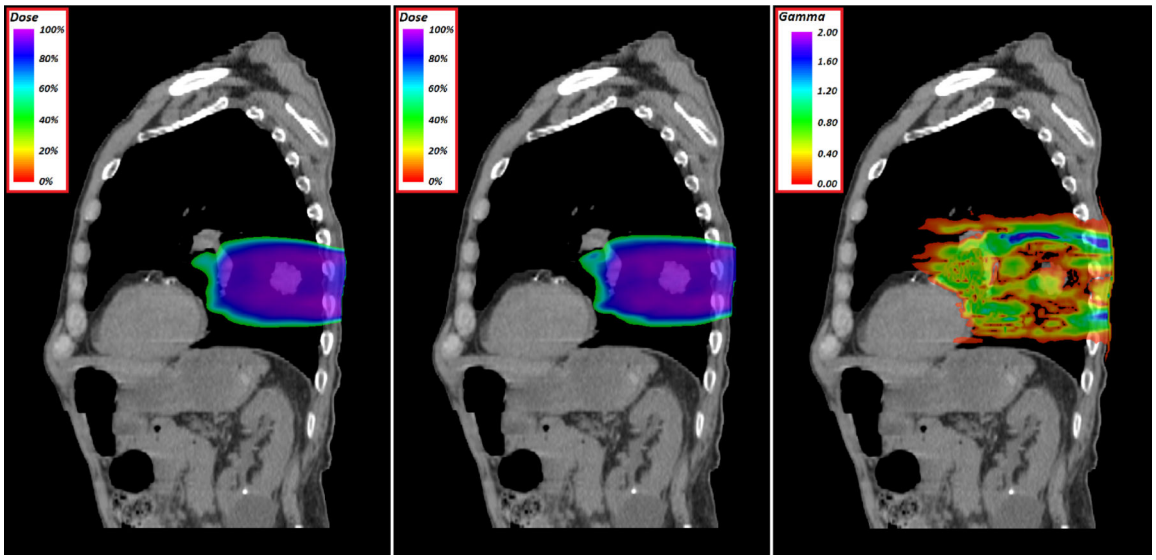

FIG. 7.

(Left) Ground truth dose using T50 as the reference CT. (Center) WED calculated dose. (Right) Global gamma analysis using 3%, 3 mm.

TABLE I

Table summarizing the gamma results of all phantom and patient data calculations.

	Tumor Motion	Gamma	Additional Notes
Phantom	*No input signal*	97.8%	*Control case - single phase*
	2 cm sinusoid	95.7%	-
	2 cm sinusoid with 3 cm drift	95.7%	-
Patient	*8.0 mm peak-to-peak*	90.8%	-
	8.0 mm peak-to-peak (Non-WED)	69.1%	*Cartesian Method*

Phantom gammas are computed with a 2 mm, 2% threshold, and patient gammas with 3 mm, 3%. “Cartesian Method” refers to the naive calculation, in which we disregarded proton range effects and performed convolutions in Cartesian space.